Chemical Concepts

International Journal of Chemical Concepts
ISSN:2395-4256 www.chemconsai.com
Vol.02, No.01, pp 01-11, 2016

Ethanol sensing performance of nanostructured Zn doped $CdSnO_3$ thin films

R. H. Bari[1]* and S. B. Patil[1]

[1]*Nanomaterials Research Laboratory, Department of Physics, G. D. M. Arts, K. R. N. Commerce and M.D. Science College, Jamner 424 206, Maharashtra, India.

Abstract: In present investigation, nanostructured $CdSnO_3$ and Zn doped $CdSnO_3$ were deposited onto heated glass substrate by simple spray pyrolysis (SP) technique. Sensing elements of nonostructured $CdSnO_3$ and Zn doped $CdSnO_3$ were annealed at 500 ^{0}C for 1 hrs. Characterization includes a different analytical technique such as, X-ray diffaractogram (XRD), energy dispersive X-ray analysis (EDAX), Field emission scanning electron microscope (FE-SEM), Transmission electron microscope (TEM) and UV–VIS absorption spectroscopy. The average crystallite size and grain size observed from XRD and FF-SEM was found to be increased with increase in volume % of Zn in $CdSnO_3$. The films volume 5 % of Zn in $CdSnO_3$ was observed to be most sensitive (S = 1230) to ethanol for 500 ppm at 300 ^{0}C. The response and recovery time is 5 sec, 7 sec respectively. The results are discussed and interpreted.

Keywords: Spray pyrolysis techniques, Nanostrutured Zn doped $CdSnO_3$, ethanol gas, response and recovery time.

1. Introduction

The nanostructured thin films are sensitive to change in their environment. Nanostructured thin film is successfully used as gas sensor due to the dependence of the electrical conductivity on the ambient gas composition [1]. Research and development of gas-sensing devices is in the focus of activity of scientists and engineers in many countries. Gas sensors can be manufactured using different materials, technologies and phenomena. Sensing devices should be smaller and cheaper hence research regarding sensitivity, selectivity, response-recovery time, reproducibility, cost, portability, deposition techniques, fabrication of devises, operating temperatures and gas concentration for different materials and gases is necessary[2]. In recent year, perovskite-type $CdSnO_3$ thin film can be used as a new type of gas sensitive materials for detecting hazardous gases. Liu and Patil et al reports the surface modifications of $CdSnO_3$ thick and thin film with Pt and Zn were also found to enhance sensitivity towards ethanol, 2-CEES and Chemical Warfares [3-5]. We reported that the surface modified perovskite-type oxide $CdSnO_3$ semiconductor could be used as a new material for detecting reducing gases such as ethanol. Semiconductor metal oxide gas sensors improve their gas response and response, recovery time due to nanocrystalline nature of the material associated, which is the most attractive quality of nanomaterials. Basically the improvements are because of the high surface area to volume ratio and smaller crystallite size compared to conventional microcrystalline materials [6].

Perovskite oxides are particularly attractive for high temperature applications. Also, the perovskite structure has two differently-sized cations, which makes it amenable to a variety of dopant additions. This doping flexibility allows for control of the transport and catalytic properties to optimize sensor performance for particular applications [7]. In order to improve the selectivity, sensitivity or gas response for a particular application, surface modification by proper choice of additives or dopants to the base materials is often used.

The doping is generally based on the selection of most effective catalysts, which modulate specific chemical reaction on the semiconductor oxide surface. Zinc, well known as an active catalyst, has been confirmed to possess the promoting effects on many semiconductor gas sensors.

In present work we have modified the surface of $CdSnO_3$ thin films using Zn catalyst to improve gas sensing performance. Therefore, spray pyrolysis technique was employed to prepare pure and Zn doped $CdSnO_3$ thin films because the technique is simple and involves low cost equipments and raw materials. The technique involves a simple technology in which an ionic solution (containing the constituent elements of a compound in the form of soluble salts) is sprayed over heated substrates [8]. By this method, dopants can be easily introduced into the matrix of the film by using appropriate precursors [9]. Additives or dopants enhance the properties of the sensors, such as gas response, selectivity, lowering the operating temperature, response and recovery time etc. [10-12].

2. Experimental

2.1 Preparation of pure nanostructured $CdSnO_3$ thin films

Aqueous solutions (0.05 M) of $CdCl_2$. $2H_2O$ and $SnCl_4 \cdot 5H_2O$ in 1:1 proportion were chosen for preparation of the thin films. The solution was sprayed at around 350 $^oC \pm 10\ ^0C$ and obtained thin film was referred as pure $CdSnO_3$. The detailed preparation of nanostructured $CdSnO_3$ using the spray system has been discussed in elsevier [13].

2.2 Preparation of nanostructured Zn-modified $CdSnO_3$ thin films

As prepared mixture (equal volume proportion 1:1) of precursor solution of cadmium acetate dehydrates (0.05M) and tin (II) chloride dehydrate with doping solution of zinc acetate dyhydrate (0.05M) in mentioned percentage variation was sprayed through a glass nozzle of 0.1 mm bore diameter, on heated glass substrate at 350 $^oC \pm 10\ ^0C$ temperature with constant flow spray rate 5 ml/min by means of air as a carrier gas. Thus the modified films of 20 min spraying time with different dopant volume (% Zn): 3, 5 and 7 were obtained and referred to B1, B2, and B3 respectively. Optimized parameters for the spray deposition of nanostructure pure $CdSnO_3$ and Zn doped $CdSnO_3$ thin films were tabulated in Table 1.

2.3 Optimized parameters

Table 1: Process parameters for the spray deposition of nanostructure $CdSnO_3$ and Zn doped $CdSnO_3$ thin films.

Spray parameter	Optimum value / item
Nozzle	Glass
Nozzle to substrate distance	30 cm
Cadmium chloride dehydrate& Tin (IV) chloride pentahydrate solution concentration	0.05M
Zinc acetate dehydrate solution concentration	0.05M
Volume % of Zn	3, 5, and 7
Spray deposition time	20 min.
Solvent	Deionised water
Solution flow rate	5 ml/ min.
Carrier gas	Compressed air
Substrate temperature	350 ^oC

2.4 Post preparative treatment (annealing)

As the prepared nanostructured pure $CdSnO_3$ and Zn doped $CdSnO_3$ thin film samples were annealed at 500 ^oC for 1 hour.

3. Characterizations

The crystal structure of thin films was analyzed with X-ray diffractometer (Miniflex Model, Rigaku, Japan, Advanced D8) by using Cu-Kα lines (λ= 1.542Å). Surface morphology was examined by means of field emission scanning electron microscope (FE-SEM Hitachi S 4800) coupled with EDAX. Microstructure property was studied using transmission electron microscopy (TEM, TECNAI $G^2$20 –TWIN FET, NETHERLAND: CM 200 Philips 200 kV HT). Optical band gap studies were conducted using UV–VIS absorption spectroscopy (Shimadzu 2450 UV-VIS). Measurement of thermoelectrical power was conducted using TEP set up (Made-Pushpa agency-Hydrabad). Electrical conductivity and gas sensing properties were checked using a static gas sensing system for different conventional gases.

4. Results and Discussion

4.1 Struactural studies

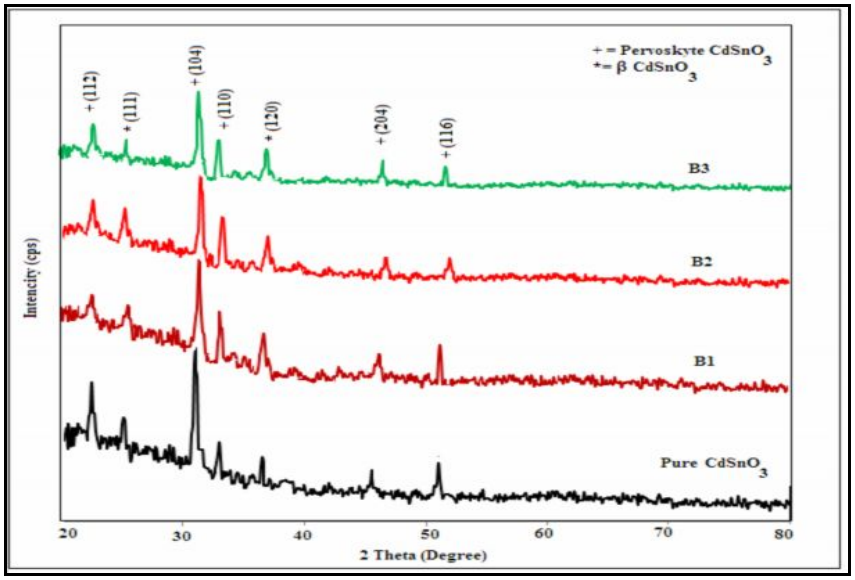

Fig. 1. X-ray diffractogram : (a) pure $CdSnO_3$ and (b) Zn doped $CdSnO_3$ (B1,B2 and B3) nanostructured thin film.

Fig. 1 shows the X-ray diffractogram of pure $CdSnO_3$ and Zn doped $CdSnO_3$(B1,B2 and B3) annealing at 500 ^{0}C. XRD recorded for the films in this work confirms the formation of mixed phase of pervoskyte (+) and β–$CdSnO_3$ (*) phase. Thin films when compared with the corresponding JCPDS data for $CdSnO_3$ (JCPDS data card no. 34- 0758, 34- 0885). In the present investigation, the films exhibit a preferential orientation along the (104) diffraction plane. No diffraction peaks from any other impurities are observed. The increase of peak sharpness indicate that the amount of the crystallite phase increases continuously with increasing volume percentage (3-5%) of Zn in $CdSnO_3$.

The variation of percentage of Zn in $CdSnO_3$ does not affect the preferred orientational growth of the films. The information on the crystallite sizes of the deposited films has been obtained using Scherer's formula [13] and it is tabulated in Table 3.

4.2 Morphological studies

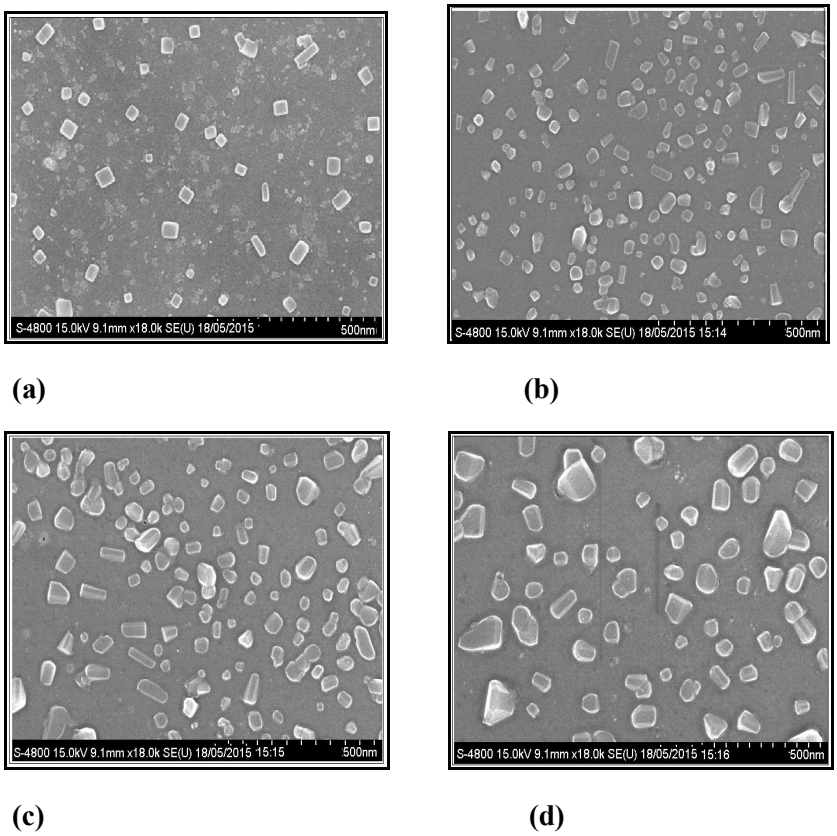

Fig. 2(a-d). FESEM morphology of deposited nanostrutured pure $CdSnO_3$ (a) and Zn doped $CdSnO_3$ (b-d) thin films.

Fig. 2 (a) shows the cubic formation of the grain for pure $CdSnO_3$ and for Zn doped $CdSnO_3$ (b-d) grains were observed to be cubic and monoclinic in shape with different size. By increasing Zn % in $CdSnO_3$ (Fig.2 (b) (c) and (d)) thin films, the shape of the grains change into the mixed cubical and monoclinic phases. Grain size observed to be in the range of 26 - 31 nm.

4.3 Elemental compositional studies

The quantative elemental composition of the spray deposited pure $CdSnO_3$ and Zn doped $CdSnO_3$ thin films on glass substrate was carried out using EDAX. The quantative elemental composition of pure $CdSnO_3$ and Zn doped $CdSnO_3$ thin films were given in Table 2.

Table 2: Quantative elemental analysis as prepared pure $CdSnO_3$ and Zn doped $CdSnO_3$ thin film.

Element	Observed							
	S1		S2		S3		S4	
	mass %	at %	mass %	at %	mass %	at %	mass %	at %
Cd	14.33	23.94	28.44	16.35	25.25	15.77	22.13	17.33
Sn	35.49	17.90	31.23	28.45	30.51	29.89	27.89	28.36
Zn	-	-	10.15	00.06	12.75	00.11	17.61	00.14
O	50.18	58.16	30.18	55.14	31.49	54.23	32.37	54.17
Total	100.00	100.00	100.00	100.00	100.00	100.00	100.00	100.00

Table 2 indicates that the formation of $CdSnO_3$ and Zn doped $CdSnO_3$ films. The at % of constituents cations and anions in the $CdSnO_3$ and Zn doped $CdSnO_3$ thin films are not as per the stoichiometric proportion i.e. films are nonstoichometric in nature. It is clear from table 6.11 that, the atomic % of Zn increases by increasing % of Zn in $CdSnO_3$ thin films. It was observed that all the samples have oxygen deficiency. This deficiency could be attributed to the larger oxygen adsorption capability of the samples. This oxygen deficiency may make the sample possible to adsorb a large amount of oxygen species favorable for high gas response.

4.4 Microstructural studies

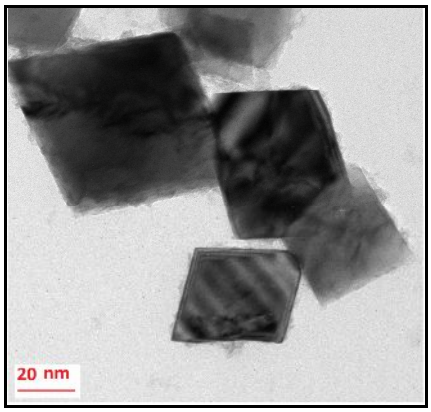

Fig. 3. TEM images of the nanostructured of most sensitive thin sample =B2

It is clear from TEM image (From fig. 3) that the grains are cubical in shape with nanocrystalline in nature. Grain size was observed to be 23 nm.

4.5 Optical band gap studies

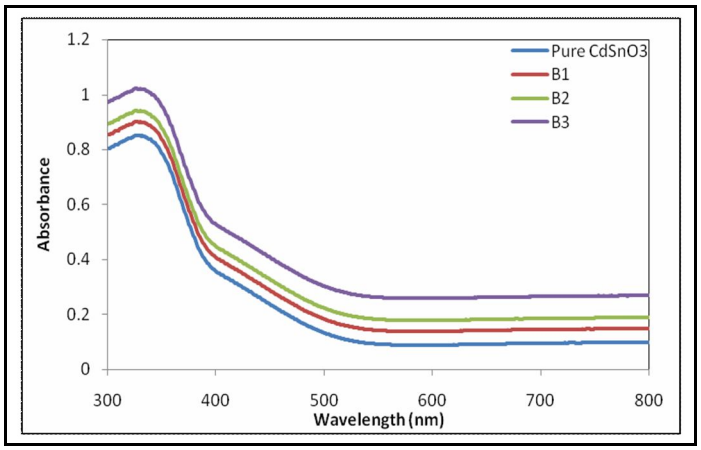

Fig. 4. The variation of relative absorbance with wavelength (nm) for nanostrutured pure $CdSnO_3$ and Zn doped $CdSnO_3$ (B1-B3) thin films.

The optical absorbance of the pure $CdSnO_3$ and Zn doped $CdSnO_3$ films formed with different wavelength of the films is shown in Fig.4. Calculated band gap energy given in Table 4. In Fig. 4 shows the absorbance spectra of thin films of samples pure $CdSnO_3$, B1, B2, and B3. The nature of the absorbance for all samples would be seems to nearly same. The band gap energies of the samples were calculated from the absorption edges of the spectra. The slope drawn from the start of an absorption edge (the onset of absorbance) and horizontal tangent had drawn on absorption minimum and intercepted each other at some point. The vertical line drawn from this point on wavelength axis gave the absorption edge wavelength [14].

This value of λ (nm) was then used in the following relation to know band gap energy:

$Eg = h\nu = h\,c/\lambda = (1240)/\lambda$ (nm) eV ----------(1)

The band gap energy calculated form absorbance spectra are 3.05, 3.12, 3.21, and 3.26 eV respectively. The band gap of thin film samples was observed to be enhanced as compared to the reported band gap 3.0 eV [15]. It may be due to nanocrystalline nature of the film.

5. Electrical Properties of the Pure and Modified Sensor

i) Thermoelectric power (TEP) measurements

The n-type semiconductivity of $CdSnO_3$ and Zn doped $CdSnO_3$ thin film samples was confirmed by measuring thermo-electromotive force of thin film sensor.

ii) I-V characteristics

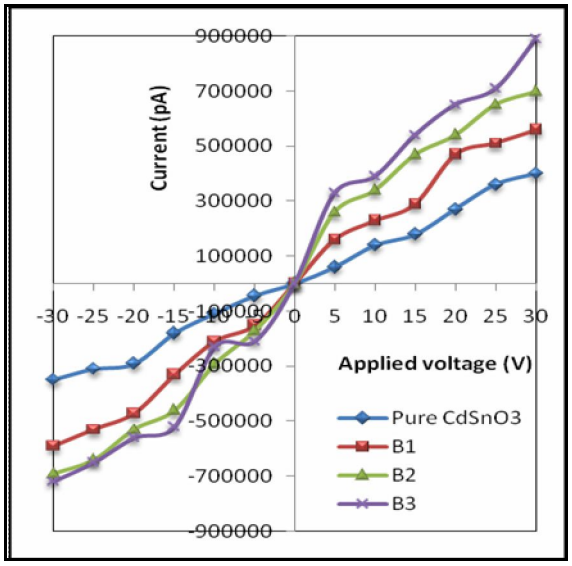

Fig. 5. I-V characteristics of nanostructured thin film sensors.

Fig. 5 shows I-V characteristics of pure $CdSnO_3$ and Zn doped $CdSnO_3$ are observed to be linear and symmetrical in nature, indicating the ohmic nature of silver contacts.

iii)Electrical conductivity

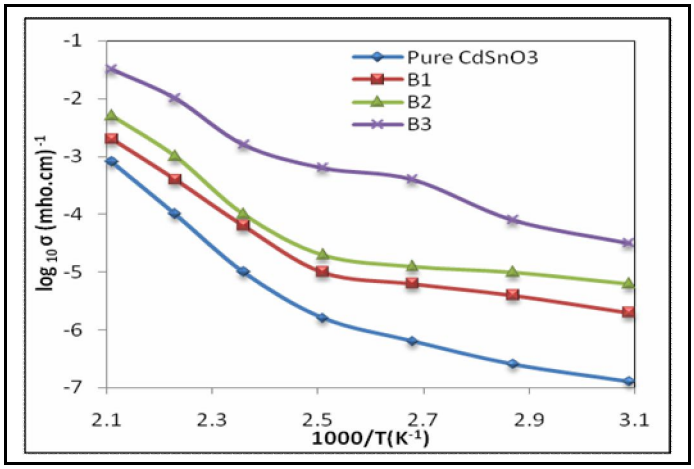

Fig. 6. Electrical conductivity of nanostructured thin film sensors.

Fig. 6 depicts the conductivities of pure $CdSnO_3$ and Zn doped $CdSnO_3$ at different operating temperature. The conductivity of Zn doped $CdSnO_3$ film was observed to be too much higher than that of pure $CdSnO_3$. This could be attributed to the Zn doped $CdSnO_3$ intergrain boundaries and hence intergranular

potential barrier [16]. It was observed that conductivity of these films goes on increasing with an increase in temperature. Hence resistivity goes on decreasing with increase of temperature.

Therefore, pure $CdSnO_3$ and Zn doped $CdSnO_3$ material exhibit negative temperature coefficient of resistance (NTC).

Electrical conductivity was calculated using the relation:

$\sigma = \sigma_o \exp(-\Delta E/kT)$ ---------- (2)
Where, σ = conductivity
σ_o = conductivity constant
k = Boltzmann constant
T = Temperature

Activation energy (Δ E) was calculated from slope of log (σ) versus inverse of temperature curve at high and low temperature range. Activation energy was represented in table 3.

Table 3: Measurement of Zn content, crystallite size, grain size, optical band gap energy and activation energy.

Sample	Zn %	Crystalline size from XRD (nm)	Grain size from FESEM (nm)	Optical band gap energy eV	Activation energy ($\triangle$ E) eV
Pure $CdSnO_3$	-	18	26	3.05	0.23
B1	3	20	27	3.12	0.21
B2	5	21	29	3.21	0.19
B3	7	24	33	3.26	0.17

Table 3 shows the crystallite sizes, grain sizes, optical band gap energy and activation energy measured from XRD, FESEM, UV-spectroscopy and electrical conductivity profile respectively. It is clear from table that the crystallite sizes, grain sizes, band gap energy goes on increasing with increase in volume % Zn in $CdSnO_3$ thin films while activation energy decreases. It may be due to the change in surface structure of the prepared thin films and formation of nanocrystalline nature [17].

6. Sensing Performance of Pure and Zn-Modified Thin Film Sensors

(i) Gas response with operating temperature

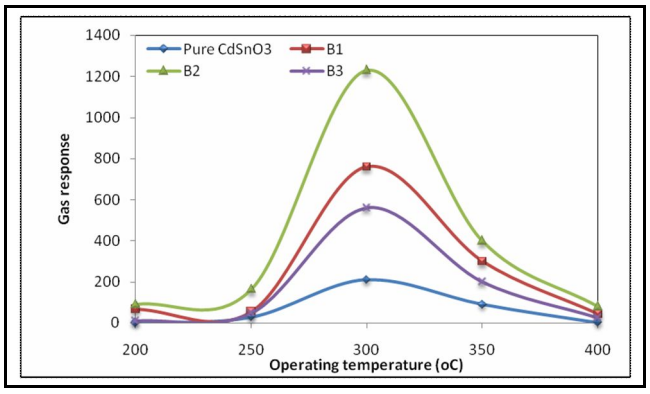

Fig. 7. Representing variation of gas response with operating temperature ^{0}C

Fig. 7 shows variations in gas response to ethanol gas (500 ppm) with operating temperature of the pure $CdSnO_3$ and Zn doped $CdSnO_3$ thin films. The gas response value of pure $CdSnO_3$ and Zn doped $CdSnO_3$ thin films were examined at various operating temperatures ranging from 200- 400 ^{o}C. The response to ethanol gas

goes on increasing with the amount of Zn, attains its maximum at 300 °C and decreases further. The largest gas response(S=1230) in case of sample with the optimum amount of Zn (vol 5%) may be because of adequate number of available sites for the oxygen to adsorbed and in turn the ability to reduce the exposed gas fastly. However, the decrease in response may be due to insufficient number of misfits (Zn) available on the surface to act as a catalyst.

(ii) Selectivity

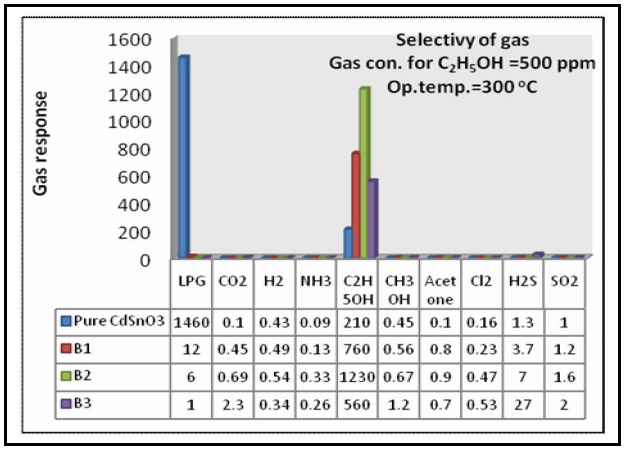

	LPG	CO2	H2	NH3	C2H5OH	CH3OH	Acetone	Cl2	H2S	SO2
Pure CdSnO3	1460	0.1	0.43	0.09	210	0.45	0.1	0.16	1.3	1
B1	12	0.45	0.49	0.13	760	0.56	0.8	0.23	3.7	1.2
B2	6	0.69	0.54	0.33	1230	0.67	0.9	0.47	7	1.6
B3	1	2.3	0.34	0.26	560	1.2	0.7	0.53	27	2

Fig. 8. Selectivity profile of nanostructured pure and Zn doped $CdSnO_3$ against various gases

Fig. 8 shows the bar diagram indicating the selectivity of pure $CdSnO_3$ and Zn doped $CdSnO_3$ sensors operated at 300 °C to ethanol gas for 500 ppm. Pure $CdSnO_3$ shows maximum gas response towards LPG gas at 350 ^{0}C. As increasing vol % of Zn in $CdSnO_3$ shifting the gas sensing performance was observed it may be due to the different absorption and deabsorption of gase molecule on the surface of $CdSnO_3$. It was observed that, doping improved selectivity of the sensor.

(iii) Response and recovery time of the sensor

The response and recovery profiles of most sensitive sensor are represented in Fig. 9. The response of the sensor was quick (5 s) and the recovery was also fast (7 s).

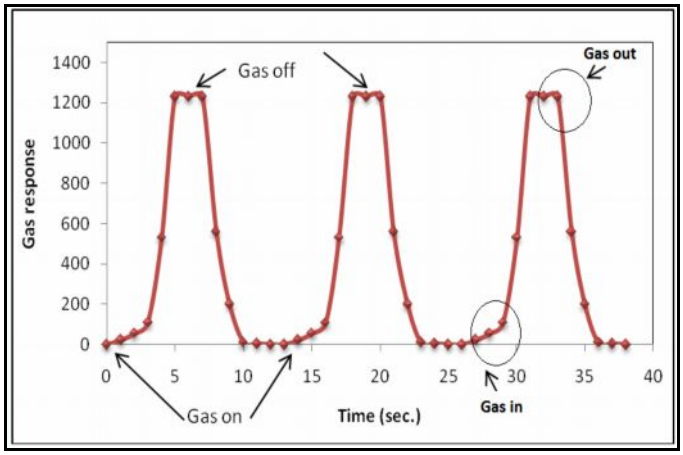

Fig. 9. Response and recovery time of (Most sensitive=B2) thin film sensor.

The fast response may be due to faster oxidation of the ethanol gas. Such a rapid response and recovery property could be attributed to the excellent electronic sensitization and catalytic activities of Zn ions. The negligible quantity of the surface reaction product and its high volatility explains its fast response and quick recovery to its initial chemical status.

iv) Stability of sensor

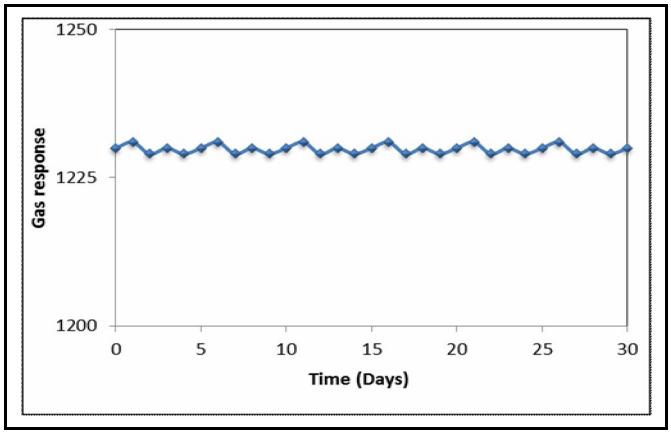

Fig.10. The long term stability profile for nanostructured Zn doped $CdSnO_3$ (most sensitive sample=B2) thin film.

The stability of the nanostructured Zn doped $CdSnO_3$ sensor were measured by repeating the test many times (30 days). During the test, no significant variation was observed as shown in Fig. 10. The ethanol gas sensor had prominent long term stability in atmosphere for about 30 days. The obtained results show that both ethanol response and electrical conductance were reproducible.

v) Comparison of ethanol response of reported sensors with sensor prepared in the present work

Table 4. Comparison of ethanol response with previous work.

Form of material/ sensor	Synthesis method	Gas conc. (ppm)	Gas response/ Sensitivity	Operating Temperature (^oC)	Reference
$CdSnO_3$ (Thin form)	Spray method	500	1230	300	Present work
$CdSnO_3$ (Thin form)	Spray method	100	576.2	200	18
$CdSnO_3$ (Thin form)	Coprecipitation method	200	68	340	19
$CdSnO_3$ (Thick form)	Solid-state reaction method	50	68.2	200	20
$CdSnO_3$ (Thin form)	Coprecipitation method	50	51	240	21
$CdSnO_3$ (Thin form)	Coprecipitation method	100	275	225	22

Table 4 presents comparison of ethanol response with reported different sensor and sensor prepared in present investigation [18–22]. It is clear that response of sensor reported in the present work is extremely high as compared to previous reported sensors.

7. Discussion

i) Ethanol gas sensing mechanism

It is well known that the gas sensing mechanism is generally explained in terms of change in conductance due to the interaction of test gases with the semiconducting surface [23]. The change of conductance is either by adsorption of atmospheric oxygen on the surface and/or by direct reaction of lattice oxygen or interstitial oxygen with the test gases.

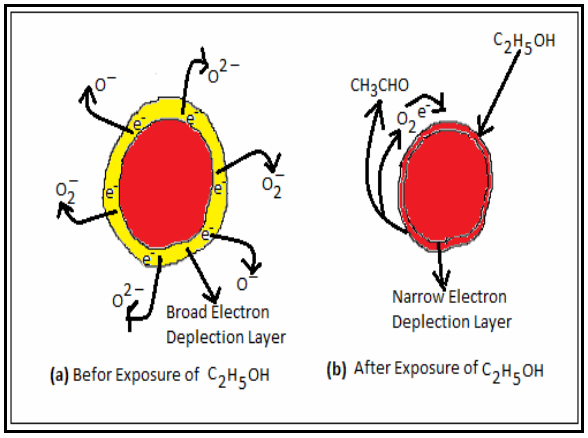

Fig. 11. Ethanol sensing mechanism of nanostructured thin film.

In case of former, the atmospheric oxygen adsorbs on the surface by extracting an electron from the conduction band, in the form of super oxides or peroxide, which are mainly responsible for the detection of the test gases. Figure 11 shows the ethanol sensing mechanism (Fig. (a) before exposure of ethanol and (b) after exposure of ethanol).

On adsorption of ethanol molecules tend to dissociate in to H atom form a surface hydroxyl and the former tends to be transformed further in to an aldehyde or a ketone. For the gas sensor to change its resistance, however, more important is the oxidation reaction of these adsorbates on the surface of nanostructured thin film. There are two general ways of ethanol conversion [24]: oxidative dehydrogenation and dehydration. For n-type semiconductor sensors the sensing mechanism is interpreted as the sensing process probably involves at three-step process, i.e., an adsorption, oxidation and desorption process is shown in Fig. 11. Before exposure of ethanol, $CdSnO_3$ nanoparticles are depleted of electrons from the conduction band by oxygen species (O_2^-, O^- and O^{2-}) adsorbed on particle surface [25, 26] forming an electron depletion layer on particle surface which increases the sensor resistance.

When the sensor is exposed to ethanol gas, the ethanol molecules are oxidized by oxygen species in to formaldehyde and simultaneously the depleted electrons are feedback in to particles, resulting in an arrowed depletion layer and therefore the sensor resistance is decreased. When gas is out, the sensor is exposed to air again and thus refreshed by air at elevated temperature. The oxygen in atmospheric air will renewably capture electrons to deplete the particle surface.

The overall chemical reaction is as follows:

$C_2H_5OH + O \rightarrow CH_3CHO + H_2O + e$ ---------- (3)

8. Conclusions

1. Spray pyrolysis technique is simple, inexpensive was successfully use for preparation of pure nanostructured $CdSnO_3$ and modified Zn doped $CdSnO_3$ thin films. It may be useful for the large scale production of nanostructured thin films.
2. The crystallite sizes were found to be in the range of ~18 nm to 24 nm.
3. FE-SEM analysis revealed that, the grains were cubical in nature and a size distribution in the range of ~26 to 33 nm.
4. EDAX analysis confirmed that the as-prepared nanostructured $CdSnO_3$ and Zn doped $CdSnO_3$ thin films was observed to be nonstoichiometric in nature.
5. TEM images showed nearly cubical crystallites with a size ~23 nm.
6. Optical study reveals that Zn doping increases the optical band gap energy varying from 3.05 to 3.26 eV.
7. As increasing vol % (3-7) of Zn in $CdSnO_3$, crystallite size, grain size and band gap energy associated with films goes on increases with decreasing activation energy.

8. Pure nanocrystalline $CdSnO_3$ thin film was observed to be the most sensitive to LPG at 350 ^{0}C. Response of Zn- $CdSnO_3$ shift towards ethanol gas observed to be higher than the response of the unmodified $CdSnO_3$ at 350 ^{0}C.Doping of Zn into $CdSnO_3$ helped to enhance the response, selectivity towards ethanol gas.
9. Speed of response (5 s) and fast recovery (7 s) are main feature of the sensor.
10. Overall it summarized that, doping improved selectivity, response and recovery time of the sensor.

Acknowledgements

The authors are thankful to the University Grants Commission, New Delhi for providing financial support. Thanks to Principal, G. D. M. Arts, K. R. N. Commerce and M.D. Science College, Jamner, for providing laboratory facilities for this work.

References

1. L.A. Patil, A.R. Bari, M.D. Shinde, V. D. Deo, *Sensors and Actuators B: Chemical,* 149, 79 (2010).
2. S.M.A. Durrani, E.E. Khawaja, M.F. Al-Kuhaili, Talanta, 65, 1162 (2005).
3. Yan-Li Liua, Yun Xingb, Hai-Feng Yanga, Zhi-Min Liua, Yu Yanga, Guo-Li Shena, Ru-Qin Yua, *Analytica Chimica Acta*, 527 (2004).
4. L.A. Patil, V.V. Deo, M.D. Shinde, A.R. Bara, M.P. Kaushik, *Sensors and Actuators B*, 160,234 (2011).
5. L. A. Patil, V. V. Deo, M. P. Kaushik, Pratibha: International journal of science, spirituality, business and technology, 1, 28 (2012).
6. G. Cadena, J .Riu, F .Rius, *Analyst*, 132, 1083 (2007).
7. J.W. Fergus, *Sens. Actuators B*, 123, 1169 (2007).
8. C .Prajapati, S.Pandey, P. Sahay, *Physica B*, 406,2684 (2011) .
9. D. Mardare, F. Iacomi, N. Cornei, M .Girtan, D.Luca, *Thin Solid Films*, 518, 4586 (2010).
10. S. Bai, Z.Tong, D. Li, X. Huang, R. Luo, A .Chen, *Sci in China Series E: Tech Sci*, 50,18 (2007).
11. G. Korotcenkov, I. Boris, A.Cornet, J. Rodriguez, A. Cirera, V. Golovanov, Y. Lychkovsky, G. Karkotsky, *Sens Actuators B*, 120,657 (2007).
12. R. Tan, Y. Guo, J. Zhao, T. Xu and W. Song, *Trans. Nonferrous Met. Soc. China,* 21, 1568 (2011).
13. R. H. Bari, S. B. Patil, A. R. Bari, *Sensors letters,* 13, 1 (2015).
14. R. H. Bari, L. A. Patil, Indian Journal of Applied Physics, 48, 127 (2010).
15. C. A. Barboza, J. M. Henriques, E. L. Albuquerque, E. W. S. Caetano, V. N. Freire, , J. A. P. da Costa, *Chem. Phys. Lett.,* 480,273 (2009).
16. V. B. Gaikwad, R. L. Patil, M. K. Deore, R. M. Chaudhari, P. D. Hire, S. D. Shinde, G. H. Jain, *Sensors & Transducers Journal*, 120,38 (2010).
17. R. H. Bari, S. B. Patil, A. R. Bari, *Optoelectronics and advanced materials – rapid communications,* 6 ,887 (2012).
18. G. E. Patil, D. D. Kajale, S. D. Shinde, N. K. Pawar, V. B. Gaikwad, and G. H. Jain, *Journal of Nanoengineering and Nanomanufacturing,* 2, 1 (2012).
19. Tianshu Zhang , Yusheng Shen , Ruifang Zhang, *Materials Letters*, 23,69 (1995).
20. Yan-Li Liua, Yun Xingb, Hai-Feng Yanga, Zhi-Min Liua, Yu Yanga, Guo-Li Shena, Ru-Qin Yua, *Analytica Chimica Acta,* 527,21 (2004).
21. Wu Xing-Hui, Wang Yu-De, Li Yan-Feng, Zhou Zhen-Lai, *Materials Chemistry and Physics,* 77, 588 (2002) .
22. Zhang Tianshu, P. Hing , Yang Li , Zhang Jiancheng, Sensors and Actuators B, 60 ,208 (1999).
23. A. P. Lee and B. J. Reedy, *Sen. and Actu.,* 60, 35 (1999) .
24. R. H. Bari, S. B. Patil, A. R. Bari, *J. of Nano. and Nanomanu*., 3,1 (2013) .
25. T. Jinkawa, G. Sakai, J. Tamaki, N. Miura, N. Yamazoe, *J. Mol. Catal. A*, 155, 193 (2000).
26. H. C. Chiu, C. S. Yeh, J. Phys. Chem.C, 111, 7256 (2007).

*****